INSTITUTE OF PHYSICS PUBLISHING JOURNAL OF PHYSICS B: ATOMIC, MOLECULAR AND OPTICAL PHYSICS

J. Phys. B: At. Mol. Opt. Phys. **39** (2006) 4155–4162 doi:10.1088/0953-4075/39/20/013

Absolute cross sections of positive- and negative-ion production in electron collision with cytosine molecules

I I Shafranyosh, M I Sukhoviya and M I Shafranyosh

Department of Physics, Uzhgorod State University, Voloshyn st. 54, Uzhgorod 88000, Ukraine

E-mail: mshafr@tn.uz.ua and lshafr@rambler.ru

Received 1 June 2006, in final form 9 August 2006
Published 10 October 2006
Online at stacks.iop.org/JPhysB/39/4155

Abstract

Production of positive and negative ions of cytosine molecules (nucleic acid base) has been studied using a crossed electron and molecular beam technique. The method developed by the authors enabled the molecular beam intensity to be measured and the electron dependences and the absolute values of the total cross sections of production of both positive and negative cytosine ions to be determined. It has been shown that the total positive cytosine ion production cross section reaches its maximal value of 7.8×10^{-16} cm^2 at the 78 eV electron energy. Dissociative ionization cross sections have also been determined. The maximum total negative cytosine ion production cross section was measured to be 4.2×10^{-18} cm^2 at 1.5 eV.

1. Introduction

Interest in experimental studies of the processes of electron-impact ion production in molecules of biological relevance is related, first of all, to the significance of the problem of intracellular irradiation of biological structures by secondary electrons produced in the substance in quite considerable amounts under the influence of a different type of radiation. Most of the secondary electrons have low energies ranging from fractions of eV to dozens of eV, and low-energy electrons are being now treated as the principal cause of destructive changes in biological structures at the molecular level. In this case genetic macromolecules are the basic target. It has been shown in our preliminary experiments carried out with the heterocyclic components of the above molecules [1–4] that under electron impact different physical processes occur: i.e., molecule excitation, ionization, dissociative excitation and dissociative ionization. The particles produced give an origin for a new cascade of physical and chemical reactions. Physical modelling of these processes and estimation of their radiobiological consequences require knowledge of their basic characteristics—absolute ionization cross sections. In this relation experimental physical modelling of ionization processes in the cells becomes topical. Intense studies of both positive- and negative-ion production in nucleic acid

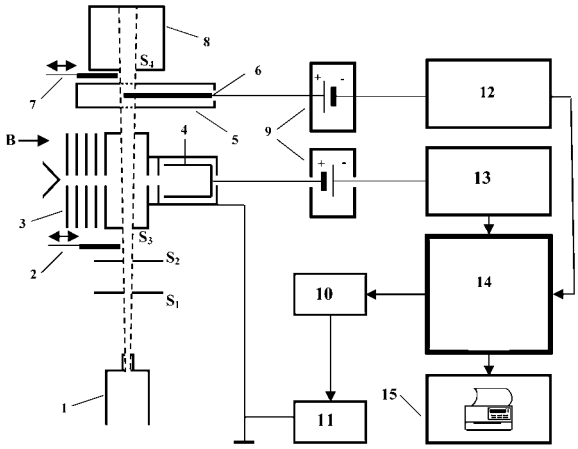

Figure 1. Experimental layout: 1, crucible; S_1–S_4, system of collimating slits; 2, 7, molecular beam flags; 3, electron gun; 4, electron collector; 5, ion collector; 6, axial electrode (probe); 8, molecule collector; 9, galvanic voltage supplies; 10, digital-to-analogue converter; 11, voltage amplifier; 12, electrometer; 13, current-to-frequency converter; 14, IBM PC AT; 15, printer.

components under slow electron impact have been carried out within the last few years [5–8]. Reliable data on the ionization cross sections could be obtained only in precise experiments, in which the role of the environment is minimized. Such an approach with the use of the crossed electron and molecular beam technique was applied in this work.

2. Experimental method and technique

The experiment was based on the crossed-beam method successfully applied by us earlier [9]. The beam of the cytosine molecules (see figure 1) was produced by means of a thermal effusion multichannel source and a system of collimating slits. This effusion source consisted of a copper container filled with a cytosine sample, a resistive container heater, a calibrated container temperature gauge (the chromel–alumel thermocouple) and thermal screens. The container was made in the form of a hollow cylinder with a special element having effusion channels (100 channels per 1.5 × 1.5 mm^2 area) mounted at one edge and a sealed cup with the cytosine sample (Sigma-Aldrich, 99% purity) and a temperature gauge at the opposite edge. The heater design ensured the microchannel element temperature was 10 K higher than that of the cup. This prevented microchannel clogging during experiment. The microchannel element produced a molecular beam with an angular divergence (aperture) of 6°. The fact that at the molecular beam boundaries a concentration gradient occurs was taken into account. The molecular beam was additionally collimated by S_1–S_3 slits (see figure 1), which selected the part of the beam with a negligibly small concentration gradient, reducing, thus, the molecular beam divergence to 4°30′.

Molecules passed the region of interaction with the electron beam and at the end of their path deposited onto the collector bottom forming with time a distinct trace—condensate. The above collector had the form of a cylindrical copper chamber with an entrance slit S_4 and a flat bottom and was kept at liquid nitrogen temperature. The mass of the condensate and time of its formation allowed the molecular beam intensity and, respectively, its concentration to be determined. The geometric size of the condensate together with the distance to the effusion source was used to determine beam parameters—i.e., the cross section in the interaction region and the angular aperture.

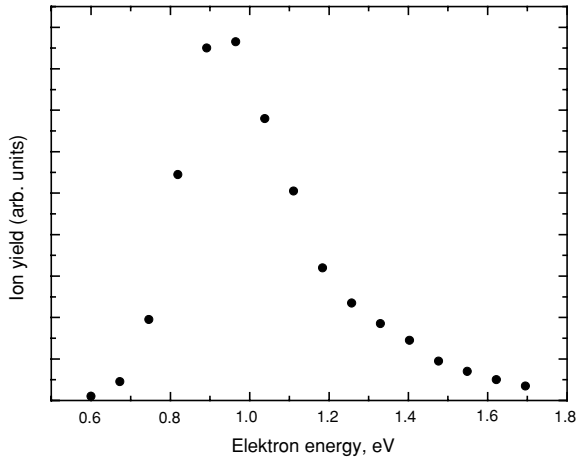

Figure 2. SF_6^- ion current versus electron energy (the contact potentials' difference was not taken into account).

A five-electrode electron gun with a thoriated tungsten cathode was used as an electron beam source. The electron gun temperature was about 400 K providing gun parameter (i.e., electron beam current, energy spread, contact voltage difference) stability during operation. The first electrode of the gun was kept at a small negative potential to retard the low-energy part of the electron flux from the cathode [10]. Electrons having passed the interaction region were trapped by a Faraday cup kept at a positive potential. Measurements were carried out at 10^{-7}–10^{-6} A electron beam current and $\Delta E_{1/2} \sim 0.3$ eV (FWHM) energy spread. The electron gun was immersed into the longitudinal magnetic field (induction $B = 1.2 \times 10^2$ T). An electron energy scale was calibrated with respect to the resonance peak of the SF_6^- ion production, the position of which determined the zero point of the energy scale.

To ensure complete collection of ions produced in the interaction region, a passthrough collector was placed on the molecular beam path with an axial electrode (probe) being mounted inside. Completeness of ion collection was provided by applying the 35 V probe voltage, the polarity of which depended on the sign of the ion charge. The magnetic field prevented collection of electrons scattered by the cytosine molecules and the electrode surfaces.

The signal detection and measurement control system included the following units: an electrometric ion current amplifier, an electron beam current-to-frequency converter, stepwise electron beam accelerating potential scanning units, a personal computer with a parallel input/out interface card and a printer. The above-mentioned system operated in the ion and electron current measuring mode at a fixed electron beam energy (to determine the absolute ionization cross section) or in the ion-to-electron current ratio measuring mode for stepwise scanning of the incident electron beam energy (to determine the energy dependence of the ionization cross section). Experiments were carried out at $\sim 1 \times 10^{-5}$ Pa vacuum.

The measuring procedure included three stages.

At the first stage the experimental technique was tested and test experiments were carried out. The collision chamber was filled with SF_6 up to 1.3×10^{-3} Pa pressure using a precise gas supply system. Then the electron gun was operated and the resonance related to the production of SF_6^- negative ions was detected. The energy position of this resonance was used to calibrate the electron energy scale, while its full width at half maximum (FWHM) was used to determine the electron beam energy spread $\Delta E_{1/2}$ (see figure 2). Then the chamber

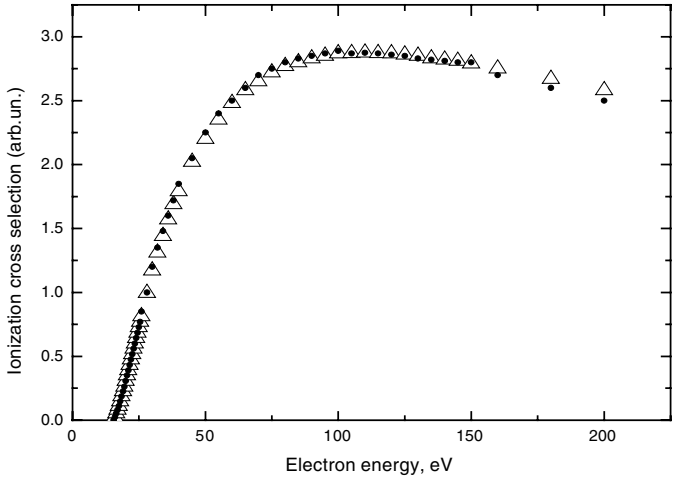

Figure 3. Total N_2^+ ion production cross section versus incident electron energy: Δ—present paper; •—data [12].

was pumped out and filled with N_2 up to 1.3×10^{-3} Pa pressure and the energy dependence of the N_2^+ ion production cross section was measured (see figure 3). A comparison of our results with the available literature data [11, 12] indicates fairly good agreement.

The measurements were carried out while varying the experimental conditions. The molecular beam concentration in the collision range was varied from 2×10^{10} cm^{-3} to 8×10^{10} cm^{-3}, while the electron beam current was varied within the (10^{-7}–10^{-6}) A range. A linear dependence of the produced ion current on the incident electron beam current and molecular target concentration was observed within the limits of the experimental error.

At the second stage the chamber was pumped out to 1×10^{-5} Pa pressure and the molecular beam source was operated (flag 2 open, flag 7 closed). The energy dependence of the positive cytosine ion production cross sections was measured (the ion-to-electron current ratio was measured via stepwise incident electron energy scanning).

At the third stage absolute values of the total negative-ion production cross sections for cytosine molecules were measured using the following relation:

$$\sigma = i/i_e nl, \tag{1}$$

where σ is the total ion production cross section; i is the relevant ion current; i_e is the electron beam current; n is the cytosine molecule concentration in the beam intersection region; and l is the electron path in the molecular beam. In the case of positive ions the absolute cross section was determined at 100 eV energy, while in the case of negative ions 5 eV was used.

It is seen that formula (1) contains those experimental parameters, the precise measuring of which is a difficult task. Especially this relates to the molecule concentration in the interaction region. Note that both i and i_e currents were measured with open flags 2, 7 (see figure 1). The cytosine-filled container temperature was elevated to 384 K and then stabilized. The time of the condensate formation in the collector was varied in five experimental cycles from 1×10^3 s to 3×10^3 s. The condensate was dissolved in distilled water after completion of the experiment and the optical density of the solution was measured in the UV region ($\lambda \sim 260$ nm). Based on the optical density value the mass of the condensate was determined.

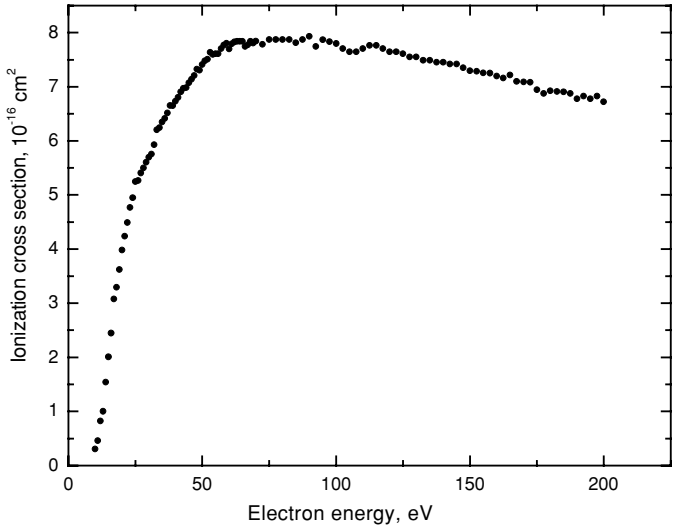

Figure 4. Total positive cytosine ion production cross section versus incident electron energy.

This mass M depends on the experimental parameters in the following way:

$$M = n\,S\,m\,v\,t, \tag{2}$$

where n is the desired concentration of the molecules in the beam intersection region; S is the collision region cross section; m is the molecular mass; v is the velocity of the molecules in the beam; and t is the condensate deposition time.

The values S and l were determined from the molecular beam geometry. Note that the incident electrons in the presence of the longitudinal magnetic field move along trochoidal trajectories, the lengths of which are, in general, larger than l. Our calculations show that due to the above effect the maximal electron path length under the conditions of our experiment (i.e., at a magnetic field induction of 1.2×10^2 T and electron gun diaphragm diameter of 1 mm) at 100 eV energy increases 1.01 times, while at 5 eV it increases 1.25 times. The relative error in determining the value n did not exceed 17%. Experiments were carried out at $n \sim 8 \times 10^{10}$ cm^{-3}. In this case the contribution due to the residual gas ionization did not exceed 2%. The results presented in this paper were obtained by averaging the data of five runs. The relative uncertainty was 9% for the energy dependences of ionization cross sections and 21% for the absolute ionization cross section values.

A similar stage-by-stage procedure was obeyed when determining the negative-ion formation cross sections for the molecules being studied.

3. Experimental results and discussions

As a result of our studies absolute values of the positive and negative cytosine ion production cross sections as well as their energy dependences were determined.

3.1. Positive ions

As seen from figure 4, the cytosine molecule ionization curve has a smooth form with weakly-pronounced features and a broad maximum in the 73–90 eV region. In particular, at 78 eV the

Table 1. Effective ionization cross sections (Q) of cytosine molecules and their fragments at 78 eV incident electron energy.

Ion	Molecular mass	Q ($\times 10^{-16}$ (cm^2)
$C_4H_5N_3O$	111	1.65
$C_4H_3N_2O$; $C_4H_5N_3$	95	0.17
$C_3H_3N_2O$; $C_3H_5N_3$	83	0.25
$C_3H_3N_3$	81	0.17
$C_4H_3N_2$	79	0.11
C_3H_3NO; $C_3H_5N_2$	69	0.52
C_3H_2NO	68	0.32
C_3HNO; $C_3H_3N_2$	67	0.36
C_2H_2NO; CN_2O	56	0.09
$C_2H_3N_2$	55	0.17
C_3H_2N	52	0.10
CH_2NO	44	0.35
CHNO	43	0.27
CH_2N_2; CNO	42	0.62
CHN_2; C_2H_3N	41	0.36
C_2H_2N	40	0.40
C_2HN	39	0.16
COH	29	0.12
CO; CH_2N	28	0.60
CHN	27	0.12
H_2O	18	0.14
OH	17	0.11
O; NH_2	16	0.12

ionization cross section value is $(7.8 \pm 0.8) \times 10^{-16}$ cm^2. The cross section measured in this work is a total cross section, i.e., it includes the positive-ion production cross section for both the initial molecule and its fragments (dissociative ionization cross sections). The positive-ion production threshold value is 9.0 ± 0.2 eV and agrees well with the data obtained by other methods [13, 14].

Of the structural features in the ionization curve which go beyond the statistical error, one may distinguish reliably the following: the shoulder at ~32 eV and a small maximum at ~110 eV. We assume that these two features are related to the dissociation ionization.

Mass-spectrometric data obtained earlier by us [2] were used to determine the cross sections of the cytosine molecule dissociative ionization product yields. Cross sections of the positive-ion production for the most probable cytosine molecule fragments at 78 eV incident electron energy are shown in table 1. The analysis of these data shows that the maximum value is observed just for the initial molecule ionization, i.e., $(1.6 \pm 0.2) \times 10^{-16}$ cm^2 at 78 eV. Ion fragment production cross sections are much smaller, i.e., 10^{-17}–10^{-18} cm^2. From the molecular fragments (see table 1), a relatively large ion-production cross section is observed for the –N–C–NH_2, –N–C=O group ions. Molecular ions not containing groups –NH_2 and –C=O as well as the pyrimidine-ring ion were also observed.

3.2. Negative ions

Energy dependence of the cytosine negative-ion production cross section is shown in figure 5. As seen, the negative cytosine ion formation has a resonance character with a maximal contribution at 1.5 eV. The maximum value of this cross section, according to our

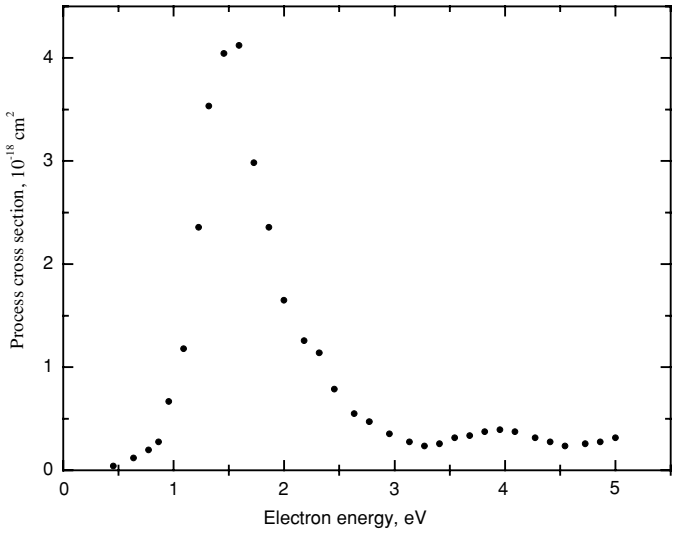

Figure 5. Total negative cytosine ion production cross section versus incident electron energy.

measurements, is 4.2×10^{-18} cm^2. The measured effective cross section is the total cross section consisting of the negative-ion production cross sections for both the initial molecule and its fragments. In addition, according to the general physical notions related to the conservation laws [15], the initial molecular ion must be produced in the excited (electronically or vibrationally) state, which, due to its instability, may dissociate into neutral and charged fragments. In the low incident electron energy range, as in our case, the most probable neutral fragments should be hydrogen atoms with the lowest binding energies in the pyrimidine ring of the cytosine molecule [13]. Thus, the negative-ion formation may proceed in two stages:

$$e + C_4H_5N_3O \rightarrow [(C_4H_5N_3O)^-]^* \rightarrow (C_4H_4N_3O)^- + H. \tag{3}$$

However, at large concentrations of the particles (e.g., in the conditions of a living cell), the probability of stabilization of the negative molecular ions due to collisions with other particles will be large.

In [16], the cytosine negative-ion production cross section at 1.54 eV (i.e., the maximum value) is 55 times larger than that obtained by us. The reason for such a discrepancy in the experimental data is not clear at the moment. One should note only that in [16] the cross section was determined by calibrating the measured data to the known negative SF_6^- ion production cross section, while in the present paper all the values required for determining the cross section were found experimentally.

One may note an additional proof of the lack of systematic error source in our experiments. Provided constant experimental conditions the ratio of the positive- and negative-ion currents is (according to (1))

$$i^+/i^- = i_e(100) \times \sigma^+(100)/i_e(4.5) \times \sigma^-(4.5), \tag{4}$$

where i^+ and i^- are the positive-ion and the negative-ion currents at the 100 eV and 4.5 eV energies, respectively; $i_e(100)$ and $i_e(4.5)$ are electron beam currents at the 100 eV and 4.5 eV energies, respectively; and $\sigma^+(100)$ and $\sigma^-(4.5)$ are the effective positive-ion (at 100 eV) and negative-ion (at 4.5 eV) formation cross sections, respectively. Thus, the above cross sections are related to each other. Increasing the negative-ion formation cross section by 1.5 orders

of magnitude results in a value of about 1×10^{-14} cm^2 for the positive-ion formation cross section, which is physically ambiguous. Since our detection system was insensitive to the ion sign, we had the possibility of controlling the ratio (4) during experiments. We have measured the i^+/i^- ratio for the case when the collision chamber was filled with SF_6. On the other hand, the ratio (4) was calculated using known positive [12] and negative [11] ion formation cross sections, as well as the experimental values of the electron beam current. The experimental and calculated data coincided within 40%.

In addition, note that our approach was reliably tested when determining the ionization cross sections for atomic systems (see [9]).

In our opinion, a profound analysis of discrepancy in the negative-ion formation cross sections should be made after the appearance of data for other nucleic bases. At present the authors are working actively with thymine and adenine molecules.

4. Conclusions

Using the technique developed by the authors, the absolute cross sections of the positive and negative cytosine ion formation have been determined within the 0–200 eV (positive ions) and 0.4–5.0 eV (negative ions) incident electron energy ranges. It has been found that the maximal positive-ion production cross section is observed at 78 eV and reaches 7.8×10^{-16} cm^2. The value of the ionization cross section obtained by us has a sense of the total cross section, i.e., it includes ion production cross sections for both initial molecules and their fragments. The formation of the primary molecular positive ion dominates. It has been found that the maximal negative-ion formation cross section is observed at 1.5 eV and is 4.2×10^{-18} cm^2. The main contribution to the cross section is likely to result from the dissociative ionization cross section. It has been noted that due to the resonance mechanism of the negative cytosine ion formation just at low incident electron energies considerable disorders in the nucleic acid macromolecules are probable.

References

[1] Sukhoviya M I and Shafranyosh I I 1987 *Elementary Processes in the Atomic and Molecular Collisions (Cheboksary)* p 121 (in Russian)
[2] Sukhoviya M I, Slavik V N and Shafranyosh I I 1991 *Biopolym. Cell.* **7** 77 (in Russian)
[3] Sukhoviya M I, Shafranyosh M I and Shafranyosh I I 1999 *Spectroscopy of Biological Molecules: New Directions* (Dordrecht: Kluwer) p 281
[4] Sukhoviya M I, Shafranyosh I I and Shimon L L 1999 *Biophys. Herald* **3** 39 (in Russian)
[5] Aflatooni K, Gallup G A and Burrow P D 1998 *J. Phys. Chem.* **102** 6205
[6] Huels M A *et al* 1998 *J. Chem. Phys.* **108** 1309
[7] Ptasinska S, Denifl S, Scheier P and Märk T D 2004 *J. Chem. Phys.* **120** 8505
[8] Ptasinska S, Denifl S, Grill V, Märk T D, Illenberger E and Scheier P 2005 *Phys. Rev. Lett.* **95** 093201–1
[9] Shafranyosh I I and Margitich M O 2000 *J. Phys. B: At. Mol. Opt. Phys.* **33** 905
[10] Fox R E 1955 *Rev. Sci. Instrum.* **26** 1101
[11] Buchelnikova H C 1958 *Zh. Eksp. Teor. Fiz.* **35** 1119 (in Russian)
[12] Rapp D and Englander-Golden P 1965 *J. Chem. Phys.* **43** 1464
[13] Verkin B I, Yanson I K, Sukhodub L F and Teplicky A B 1985 *Biomolecular Interactions. New Experimental Approaches and Methods* (Kiev: Naukova Dumka) p 317 (in Ukrainian)
[14] Steenken S 1993 *J. Am. Chem. Soc.* **114** 4701
[15] Massey H 1976 *Negative Ions* (Cambridge: Cambridge University Press) p 754
[16] Denifl S, Hanel G, Gstir B, Ptasinska S, Scheier P, Probst M, Farizon B, Farizon M, Illenberger E and Märk T D 2003 *Book of Abstr. 23rd Int. Conf. on Photonic, Electronic and Atomic Collision (ICPEAC) (Stockholm) We096*